Whole-Body PET/CT with ^{11}C-Meta-Hydroxyephedrine in Tumors of the Sympathetic Nervous System: Feasibility Study and Comparison with ^{123}I-MIBG SPECT/CT

Christiane Franzius[1], Klaudia Hermann[1], Matthias Weckesser[1], Klaus Kopka[1], Kai Uwe Juergens[2], Josef Vormoor[3], and Otmar Schober[1]

[1]Department of Nuclear Medicine, University Hospital, Münster, Germany; [2]Department of Clinical Radiology, University Hospital, Münster, Germany; and [3]Department of Pediatric Hematology and Oncology, University Hospital, Münster, Germany

The ^{11}C-labeled tracer meta-hydroxyephedrine (^{11}C-HED) is a noradrenaline analog that was developed to visualize the sympathetic nervous system with PET. Initial clinical studies show a rapid uptake of ^{11}C-HED in localized tumors of this system. Whole-body imaging with ^{11}C-HED PET is now possible as PET/CT scanners allow a rather short examination time. The aim of this study was to evaluate the feasibility of whole-body ^{11}C-HED PET/CT for examination of tumors of the sympathetic nervous system and to directly compare the results with ^{123}I-labeled meta-iodobenzylguanidine (^{123}I-MIBG) scintigraphy, including SPECT/CT. **Methods:** In 19 consecutive patients, 9 mo to 68 y old (median, 32 y), 24 whole-body ^{11}C-HED PET/CT (low-dose CT) examinations were performed. Scans were compared with attenuation-corrected ^{123}I-MIBG SPECT/CT scans (24-h scan, low-dose CT). The intensity of tracer accumulation above background was visually analyzed in both scans, PET and SPECT, using a 4-value scale. In ^{11}C-HED PET, mean and maximum standardized uptake values were determined for all lesions. **Results:** In 14 patients with 19 pairs of examinations, the following tumors were confirmed histologically: 6 neuroblastomas, 5 pheochromocytomas, 1 ganglioneuroblastoma, and 2 paragangliomas. In 5 patients, each having 1 pair of examinations, clinical follow-up and/or histologic examination did not reveal any tumor deriving from the sympathetic nervous system. ^{11}C-HED PET/CT detected 80 of 81 totally depicted tumor lesions (sensitivity, 0.99; soft tissue, 61; bone, 19). ^{123}I-MIBG SPECT/CT detected 75 of 81 lesions (sensitivity, 0.93; soft tissue, 56; bone, 19). With both methods, there were no false-positive lesions. The tumor-to-background contrast of ^{11}C-HED uptake was higher in comparison with ^{123}I-MIBG uptake in 26 lesions (0.32; soft tissue, 18; bone, 8), equal in 39 lesions (0.48; soft tissue, 30; bone, 9), and lower than ^{123}I-MIBG uptake in 16 lesions (0.20; soft tissue, 14; bone, 2). **Conclusion:** Whole-body imaging using ^{11}C-HED PET/CT is feasible in the clinical setting of patients with tumors of the sympathetic nervous system. ^{11}C-HED PET/CT detected more tumor lesions than ^{123}I-MIBG SPECT/CT. However, tumor-to-background contrast of ^{11}C-HED in lesions can be higher, equal, or lower compared with ^{123}I-MIBG.

Key Words: ^{11}C-HED PET/CT; ^{123}I-MIBG SPECT/CT; neuroblastoma; pheochromocytoma; sympathetic nervous system tumors

J Nucl Med 2006; 47:1635–1642

Neuroblastomas, pheochromocytomas, ganglioneuroblastomas, and paragangliomas are tumors deriving from the sympathetic nervous system. These tumors originate from the adrenal gland and sympathetic ganglions anywhere from the neck to the pelvis. In the case of malignant tumors, metastases can be found in soft tissue, bone, and bone marrow. Because of their neuroendocrine origin these tumors are able to take up catecholamines and related substances. The diagnosis of these tumors is established biochemically by measuring the level of urinary and plasma catecholamines and their metabolites. Today there are several morphologic and functional imaging methods available that predict tumor localization and tumor extent and give anatomic information (*1*). CT and MRI are the morphologic imaging modalities of choice in localizing these tumors (*2*). Both provide excellent anatomic details and sensitivity is very high. Both are lacking in specificity as difficulties may occur in distinguishing between tumors deriving from the sympathetic nervous system and other tumor entities (*1*). The major advantages of radionuclide imaging are high sensitivity, very high specificity, and the routinely performed whole-body scanning. Furthermore, in follow-up examinations, functional imaging is not affected by postoperative artifacts such as scar tissue or metallic clips.

The catecholamine analog ^{123}I-meta-iodobenzylguanidine (^{123}I-MIBG) is the radiotracer most widely used to image tumors of the sympathetic nervous system. With regard to

Received Mar. 16, 2006; revision accepted Jul. 17, 2006.

For correspondence or reprints contact: Christiane Franzius, MD, Department of Nuclear Medicine, University Hospital Münster, Albert-Schweitzer-Strasse 33, 48149 Münster, Germany.

E-mail: franziu@uni-muenster.de

its physical characteristics and kinetics, ^{123}I-MIBG is less than ideal for imaging. In contrast, ^{11}C-labeled metahydroxyephedrine (^{11}C-HED) is a catecholamine analog that has been developed specifically for imaging the sympathetic nervous system using PET (*3*). ^{11}C-HED uptake reflects catecholamine transport, storage, as well as catecholamine recycling (*4*). Preliminary kinetic studies suggested a rapid accumulation and high retention of ^{11}C-HED in localized neuroblastomas and pheochromocytomas (*5–7*). However, to our knowledge, whole-body ^{11}C-HED PET for the detection of extraadrenal tumors and metastases has not yet been performed in a larger patient cohort (*8,9*). Fast PET/CT hybrid scanners enable attenuation-corrected, high-quality whole-body images of radionuclides with a short half-life. The purpose of this study was to evaluate the feasibility of whole-body ^{11}C-HED PET/CT with low-dose CT in a clinical setting in all age groups and to directly compare the results with ^{123}I-MIBG single-photon emission tomography combined with low-dose CT (SPECT/CT).

MATERIALS AND METHODS

Patients

Within a 20-mo period of time, all patients with known or suspected tumors of the sympathetic nervous system who were referred for ^{123}I-MIBG scintigraphy were included in this investigation. Twenty-four pairs of examinations (^{123}I-MIBG scintigraphy and ^{11}C-HED PET/CT) were performed on 19 patients, age 9 mo to 68 y old (median, 32 y). The time interval between the ^{11}C-HED PET/CT and ^{123}I-MIBG scintigraphy was <4 wk for all examinations (median, 6 d; range, 0–25 d), and within this interval no therapy or intervention was performed. In 14 pairs of examinations, chemotherapy, ^{131}I-MIBG therapy, and/or resection of the tumor preceded the scans and the patients had recurrent or persistent disease. In 10 pairs of examinations, no therapy was performed previously. None of the patients was on medication known to interfere with the cellular uptake of catecholamines. Whenever necessary, young children were sedated or anesthetized for imaging by a pediatrician or anesthesiologist.

This investigation was approved by the local ethics committee for adults (all tumor types) and for children (neuroblastoma only). This study had to include children, as neuroblastomas do not occur in adult patients. All patients or parents (in the case of pediatric patients) gave written informed consent.

^{11}C-HED PET/CT

The synthesis of ^{11}C-HED has been previously described in detail (*4*). Patients received an intravenous injection of 320 MBq ^{11}C-HED (median; range, 125–716 MBq). In children, the injected activity was corrected for body weight starting with 370 MBq for a 70-kg individual and scaling down according to recommendations of the pediatric task group of the European Association of Nuclear Medicine (EANM). PET/CT studies were performed using a hybrid scanner (Biograph Sensation 16; Siemens Medical Solutions). Whole-body unenhanced, low-dose multidetector-row CT (MDCT) for attenuation correction and anatomic land marking was started immediately after the injection with the patients holding their breath in mild expiration (detector configuration, 16×0.75 mm; gantry rotation time, 420 ms; tube voltage, 120 kV; effective tube current, 13–20 mAs, online tube current modulation [Care Dose; Siemens Medical Solutions]; table feed, 30 mm/rotation; field of view, at least from the base of the skull to the middle of the thigh, CT parameters were adapted to body weight or axial diameter in children). Whole-body PET acquisition was started 5 min after the injection (field of view from the base of the skull to the middle of the thigh, 4-min emission scan per bed position). Data from low-dose MDCT were reconstructed in an overlapping manner at 2-mm slice thickness with a 1-mm reconstruction increment, using the standard soft-tissue reconstruction kernel B30, the lung reconstruction kernel B50, and the bone reconstruction kernel B60. Attenuation-corrected PET images were reconstructed iteratively. For CT data analysis, the window width were set to 350 Hounsfield units (HU) and the window center was set to 50 HU (soft tissue), 1,700 HU/−500 HU (lung parenchyma), and 320 HU/800 HU (bone structures).

^{123}I-MIBG Scintigraphy and SPECT/CT

^{123}I-MIBG was injected intravenously at least 30 min after blocking the thyroid gland by orally given 300 mg sodium perchlorate. In children, activity was given weight adapted according to recommendations of the pediatric task group of the EANM using 370 MBq for 70-kg body weight. Whole-body scintigraphy in anterior and posterior views, lateral views of the head, and single SPECT of the primary tumor region were performed 4 and 24 h after injection. Planar scintigraphy was acquired with a dual-head whole-body γ-camera (Bodyscan, Siemens; or Hawkeye, GE Healthcare) with a scanning velocity of 5 cm/min. SPECT was acquired with a dual-head γ-camera (Hawkeye), equipped with a medium-energy collimator. Thirty-two projections, 40 s each, were acquired over a 180° rotation in a 64×64 matrix. Low-dose CT was performed with the 24-h postinjection acquisition for attenuation correction and anatomic orientation (*10*). SPECT images without (4 h after injection) and with attenuation correction (24 h after injection) were reconstructed iteratively.

Data Analysis and Interpretation

^{11}C-HED PET and low-dose MDCT were transferred to a Leonardo workstation (VA 70; Siemens Medical Solutions) for further assessment. ^{11}C-HED PET and ^{123}I-MIBG scintigraphy were analyzed independently, each by 2 experienced nuclear medicine physicians who knew the patients' data and clinical symptoms but were unaware of other imaging results. In case of disagreement between both readers, consensus was obtained. Any focal tracer uptake in the adrenal glands or extraadrenal regions that exceeded the normal regional tracer uptake was considered a pathologic lesion. Pathologic lesions were categorized semiquantitatively using a 4-value scale (1 = faintly, 2 = moderately, and 3 = highly increased tracer uptake above background). A site was classified as 0 (no increased tracer uptake) in case a tumor manifestation was not visible with the assessed method. Analysis was performed on a computer monitor in all 3 planes of the ^{11}C-HED PET and the 24-h postinjection ^{123}I-MIBG SPECT. Furthermore, any pathologic lesion was localized by image fusion with the low-dose CT. Low-dose MDCT scans of the PET/CT were read in the soft-tissue, bone, and pulmonary window by 2 experienced radiologists. Low-dose MDCT was used to determine the size of the lesions. Additionally, in the ^{11}C-HED PET, mean and maximum standardized uptake values (SUV_{mean}, SUV_{max}) were assessed for all lesions and for normal organs. Tumor sites that were not within the field-of-view on 24-h postinjection ^{123}I-MIBG SPECT were excluded from the semiquantitative analyses and the direct

TABLE 1
Characterization of Tumor Patients

Patient*	Age (y)	Sex	Histology	Primary tumor	Metastases	Indication
BM	37	M	Pheochromocytoma	After resection	Soft tissue	Relapse, restaging
ES	40	M	Pheochromocytoma	Adrenal glands, bilateral	Soft tissue	Staging, MEN IIa
HA1	33	F	Pheochromocytoma	After resection, local relapse	Soft tissue	Relapse, restaging
HA2	33	F	Pheochromocytoma	After resection, local relapse	Soft tissue	Follow-up after operation
SI	66	F	Pheochromocytoma	Adrenal gland	No	Staging
BA	51	F	Pheochromocytoma	After resection	Soft tissue	Progression, restaging
EN	5	F	Neuroblastoma	After resection	Soft tissue, bone	Relapse, restaging
SL	4	M	Neuroblastoma	Adrenal gland/abdomen	Bone	Staging
BV1	6	F	Neuroblastoma	After resection	Soft tissue, bone	Relapse, restaging
BV2	6	F	Neuroblastoma	After resection	Soft tissue, bone	Follow-up after therapy
BR	2	F	Neuroblastoma	Adrenal gland/abdomen	Soft tissue	Follow-up after therapy
WJ	9†	M	Neuroblastoma	Adrenal gland/abdomen	No	Staging
KL	2	M	Neuroblastoma	Adrenal gland/abdomen	Bone	Staging
KS1	23	F	Ganglioneuroblastoma	After resection	Soft tissue	Relapse, restaging
KS2	24	F	Ganglioneuroblastoma	After resection	Soft tissue	Follow-up after therapy
KS3	24	F	Ganglioneuroblastoma	After resection	Soft tissue	Follow-up after therapy
OJ	59	M	Paraganglioma	After resection	Soft tissue, bone	Progression, restaging
GP1	57	M	Paraganglioma	Paravertebral	Soft tissue, bone	Progression, restaging
GP2	57	M	Paraganglioma	Paravertebral	Soft tissue, bone	Follow-up after therapy

*Number of pair of examinations if patient had >1 pair of examinations.
†Months.
MEN IIa = multiple endocrine neoplasia, type IIa.

comparison of both tomographic methods, ^{11}C-HED PET/CT and ^{123}I-MIBG SPECT/CT.

Morphologic Imaging

All patients underwent additional morphologic imaging using contrast-enhanced MDCT, MRI, or ultrasound during their clinical work-up.

Gold Standard

At least one tumor site was confirmed histologically in all tumor patients studied. In patients with multiple tumor manifestation, not all sites were verified histologically because of the advanced stage of disease and the systemic therapy as the first therapeutic choice. To clarify discrepant results between ^{11}C-HED PET and ^{123}I-MIBG SPECT, low-dose CT, the other morphologic imaging methods, and the clinical and imaging follow-up were used. If either PET or SPECT was negative in a region with a clearly visible lesion in morphologic imaging, the negative finding was considered false-negative. In case of clearly positive PET or SPECT but negative morphologic imaging, clinical and imaging follow-up were considered.

Statistics

Normal distribution was tested by the Kolmogorov–Smirnov test. Sensitivities were calculated on a lesion-by-lesion and examination-by-examination basis. The 95% confidence intervals (95% CI) are given for these parameters.

RESULTS

Fourteen patients were included in this study after histologic confirmation of the following tumors: 6 neuroblastomas, 5 pheochromocytomas, 1 ganglioneuroblastoma, and 2 paragangliomas (Table 1). These 14 patients with a total of 19 pairs of examinations constitute the study group (10 patients with 1 pair, 3 patients with 2 pairs, and 1 patient with 3 pairs of examinations). For ^{123}I-MIBG scintigraphy, a total of 6 sedations were performed (3 neuroblastoma

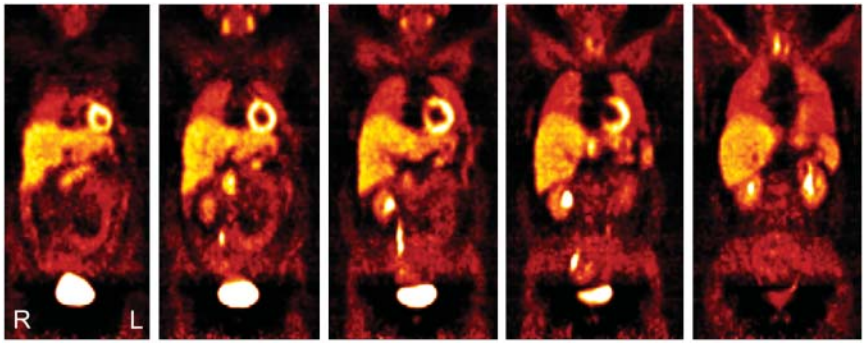

FIGURE 1. A 43-y-old woman with normal whole-body distribution on ^{11}C-HED PET scan (several levels of coronal slices) with high ^{11}C-HED accumulation in renal pelvis, ureter, urinary bladder, myocardium, liver, thyroid, and pancreas and moderate tracer uptake in salivary glands and spleen. Adrenal glands demonstrate only very low ^{11}C-HED uptake and can only be differentiated from surrounding tissue by using PET/CT fusion image.

patients, 4 and 24 h after injection). In the same 3 patients, two ^{11}C-HED PET/CT examinations were performed under sedation and 1 was performed under general anesthesia (radiotherapy planning CT in the same session).

In 5 patients referred for the evaluation of suspected pheochromocytoma and each having 1 pair of examinations, ^{11}C-HED PET/CT, ^{123}I-MIBG scintigraphy, and SPECT/CT, clinical and imaging follow-up and/or histologic examination did not reveal any tumor deriving from the sympathetic nervous system. The ^{11}C-HED PET/CT examinations of these patients were analyzed to describe the normal whole-body ^{11}C-HED distribution.

Normal Whole-Body ^{11}C-HED Distribution

With exception of the urogenital system and the thyroid gland, all 5 persons in whom no tumor of the sympathetic nervous system could be verified showed a uniform distribution pattern of ^{11}C-HED in the body (Fig. 1; Table 2). Very low tracer accumulation was shown in soft tissue, muscle, gut, lungs, and bones. Homogeneous moderate tracer accumulation was shown in salivary glands, spleen, and adrenal glands. Homogeneous high uptake was demonstrated in myocardium, liver, and pancreas. Variable high ^{11}C-HED accumulation was demonstrated in renal parenchyma, renal pelvis, ureter, urinary bladder, and thyroid gland.

Tumor Patients

Lesions Within Field of View of ^{123}I-MIBG SPECT/CT. Using ^{11}C-HED PET/CT, 80 of 81 totally detected lesions showed increased tracer uptake, 19 osseous lesions and 61 soft-tissue lesions (Tables 3 and 4). Despite the massive physiologic ^{11}C-HED accumulation in the renal collecting system and the high pancreatic ^{11}C-HED uptake, lesions next to these organs could be unequivocally differentiated in all cases by means of ^{11}C-HED PET/CT fusion images.

TABLE 2
Normal Distribution of ^{11}C-HED (n = 5)

Organ or tissue	SUV_{max}	SUV_{mean}
Salivary gland	8.8 ± 2.8	4.7 ± 0.8
Thyroid (n = 4)	12.8 ± 5.1	5.5 ± 1.6
Lung	2.5 ± 0.8	1.6 ± 0.4
Myocardium (L ventricle)	9.9 ± 2.8	5.6 ± 1.4
Liver	9.0 ± 2.7	5.3 ± 1.2
Spleen	5.0 ± 1.0	4.1 ± 0.8
Pancreas	11.5 ± 3.3	6.2 ± 1.1
Adrenal gland	4.9 ± 2.7	3.2 ± 1.7
Kidney, parenchyma	6.0 ± 1.4	4.4 ± 1.7
Kidney, pelvis	36.7 ± 8.8	13.7 ± 2.6
Ureter	15.4 ± 10.9	5.5 ± 3.9
Urinary bladder	148.7 ± 82.5	64.9 ± 20.3
Bowel	2.6 ± 0.8	1.5 ± 0.1
Vertebral body	2.8 ± 0.8	1.6 ± 0.4
Long bone	0.8 ± 0.1	0.5 ± 0.1
Muscle	1.5 ± 0.3	0.6 ± 0.2

Data are expressed as mean ± SD.

TABLE 3
Results of Imaging Procedures: Lesion-Based Analysis

Tumor or localization	^{11}C-HED PET			^{123}I-MIBG SPECT		
	TP	FP	FN	TP	FP	FN
Neuroblastoma	25	0	1*	26	0	0
Pheochromocytoma	21	0	0	17	0	4
Paraganglioma	27	0	0	26	0	1
Ganglioneuroblastoma	7	0	0	6	0	1
Osseous	19	0	0	19	0	0
Soft tissue	61	0	1*	56	0	6
Total	80	0	1*	75	0	6

*No increased ^{11}C-HED uptake in large local relapse. In low-dose CT, large tumor mass is visible.
TP = true-positive; FP = false-positive; FN = false-negative.

^{123}I-MIBG SPECT/CT 24 h after injection demonstrated a total of 75 of 81 lesions, 19 osseous lesions and 56 soft-tissue lesions. There were no additional lesions on the 4-h postinjection ^{123}I-MIBG SPECT images. There was only 1 additional lesion on ^{123}I-MIBG SPECT not showing up on the PET scan by an increased ^{11}C-HED accumulation. This lesion was a large local relapse of a neuroblastoma and was visible on the low-dose CT component of the PET/CT ($4.2 \times 4.6 \times 5.3$ cm). This positive ^{123}I-MIBG finding had a clear influence on further therapy. Six lesions in 3 patients (4 examinations) were false-negative by ^{123}I-MIBG SPECT/CT (median maximum diameter, 2.2 cm; range, 1.4–2.4 cm). Five of these lesions in 3 examinations (2 patients) led to a change of the therapeutic management (surgery). All positive lesions in both imaging procedures revealed true-positive lesions. The lesion-based sensitivity of ^{11}C-HED PET was calculated to be 0.99 (80/81; 95% CI, 0.93–1.00); sensitivity of ^{123}I-MIBG SPECT was calculated to be 0.93 (75/81; 95% CI, 0.84–0.97). Because there were no false-positive lesions, specificity could be stated to be 1.00 in both imaging techniques. Furthermore,

TABLE 4
SUVs in ^{11}C-HED PET: Lesion-Based Analysis

Lesion localization (no.)	Median or quantile	SUV_{max}	SUV_{mean}
Total (81)*	Median	8.9	4.3
	25th quantile	4.3	2.3
	75th quantile	15.0	7.9
Osseous (19)	Median	3.4	1.9
	25th quantile	2.8	1.6
	75th quantile	5.4	3.7
Soft tissue (62)*	Median	10.9	6.1
	25th quantile	5.5	3.3
	75th quantile	16.4	8.7

*SUVs were also calculated for large neuroblastoma relapse that was missed in visual analysis of ^{11}C-HED PET.

examination-based sensitivity was 1.00 (19/19; 95% CI, 0.82–1.00) in both ^{11}C-HED PET/CT and ^{123}I-MIBG SPECT/CT.

The intensity of tracer uptake (4-value score) was variable in both ^{11}C-HED PET/CT and ^{123}I-MIBG SPECT/CT when comparing different patients or different lesions in the same patients (Figs. 2–4; Table 5). Whereas in most osseous lesions the intensity of ^{11}C-HED uptake was equivalent (9/19; 0.47) or higher (8/19; 0.42) as compared with the ^{123}I-MIBG uptake, in soft-tissue lesions tracer uptake was either equivalent (30/62; 0.48), higher using ^{11}C-HED (18/62; 0.29), or higher using ^{123}I-MIBG (14/62; 0.23).

Lesions Outside Field of View of ^{123}I-MIBG SPECT/CT. In addition to the above lesions, the following lesions were found in regions outside the field of view of the ^{123}I-MIBG SPECT/CT in a total of 10 pairs of examinations in 7 patients: 9 concordant positive lesions; 16 lesions true-positive using ^{11}C-HED PET/CT and false-negative using planar ^{123}I-MIBG scintigraphy; and 5 lesions true-positive using planar ^{123}I-MIBG scintigraphy and not within the field of view of the ^{11}C-HED PET/CT (1 scull, 2 distal femur, 2 tibia).

DISCUSSION

Several imaging procedures have been used to localize tumors of the sympathetic nervous system. CT and MRI provide excellent morphologic images and offer high sensitivities in the depiction of pheochromocytomas and neuroblastomas (*1,11*) but, unless indicated, only the abdomen is scanned and, therefore, small extraabdominal tumors may be missed. Moreover, CT and MRI depict only morphologic abnormalities and cannot functionally characterize adrenal or extraadrenal masses. Widely applied whole-body ^{123}I-MIBG scintigraphy localizes neuroblastoma and pheochromocytoma with a high sensitivity and very high specificity and is extremely helpful in the detection of extraadrenal tumor sites (*1*). However, ^{123}I-MIBG scintigraphy

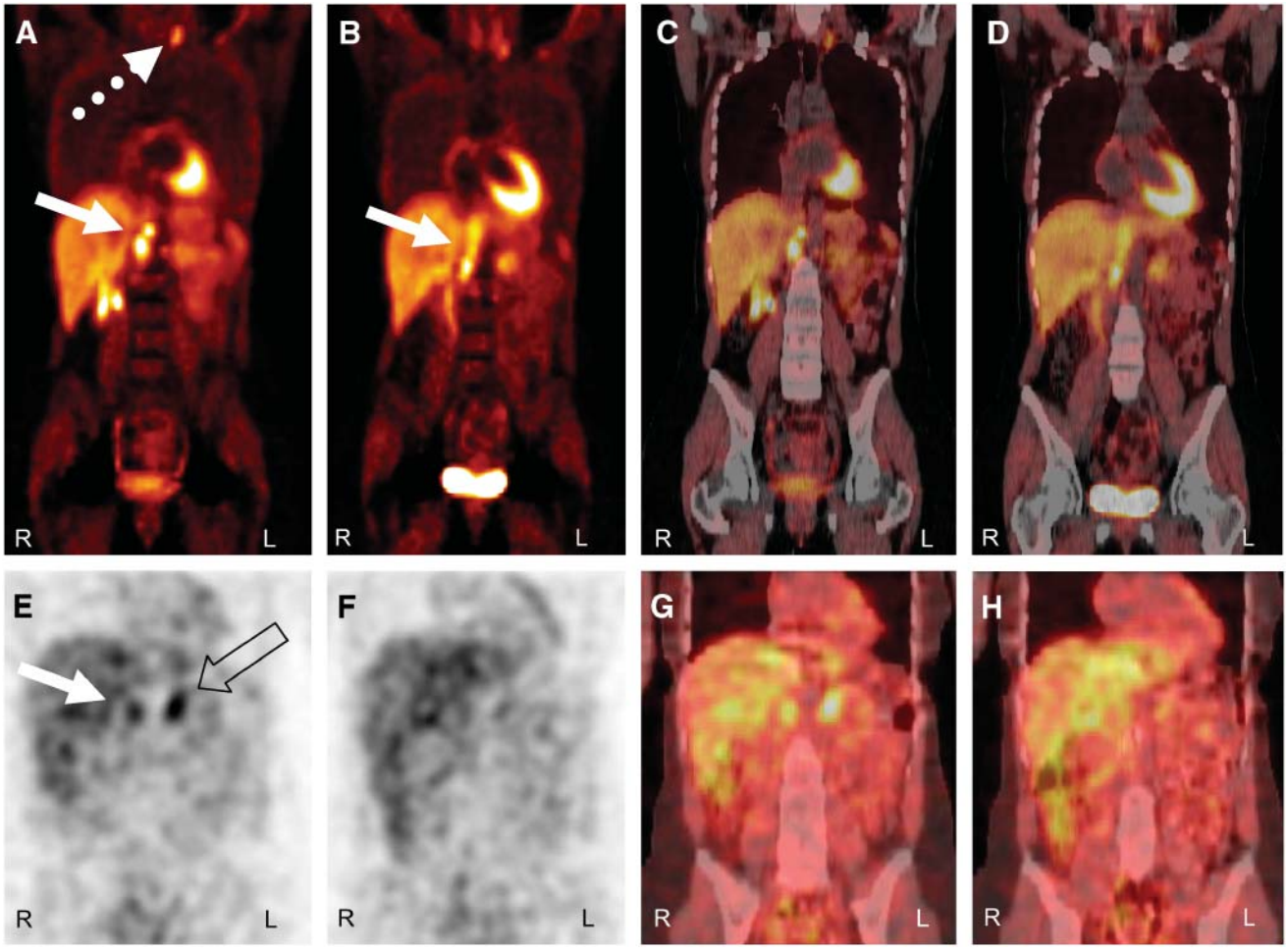

FIGURE 2. A 33-y-old woman (patient HA) who had pheochromocytoma of right adrenal gland and resection years ago. ^{11}C-HED PET/CT: (A and B) PET images; (C and D) PET/CT fusion images, 2 levels of coronal slices. There is local relapse (solid arrow) and metastases retrocrural (solid arrow), cervical (dotted arrow), and mediastinal (not shown) with highly increased tracer uptake. ^{11}C-HED uptake of left adrenal gland is very low. ^{123}I-MIBG SPECT/CT: (E and F) SPECT images; (G and H) SPECT/CT fusion images, 2 levels of coronal slices. There is moderately increased tracer uptake in local relapse (solid arrow) and physiologic uptake in left adrenal gland (open arrow). Retrocrural metastases are not visible with increased ^{123}I-MIBG accumulation. Cervical and mediastinal metastases are not within field of view of SPECT.

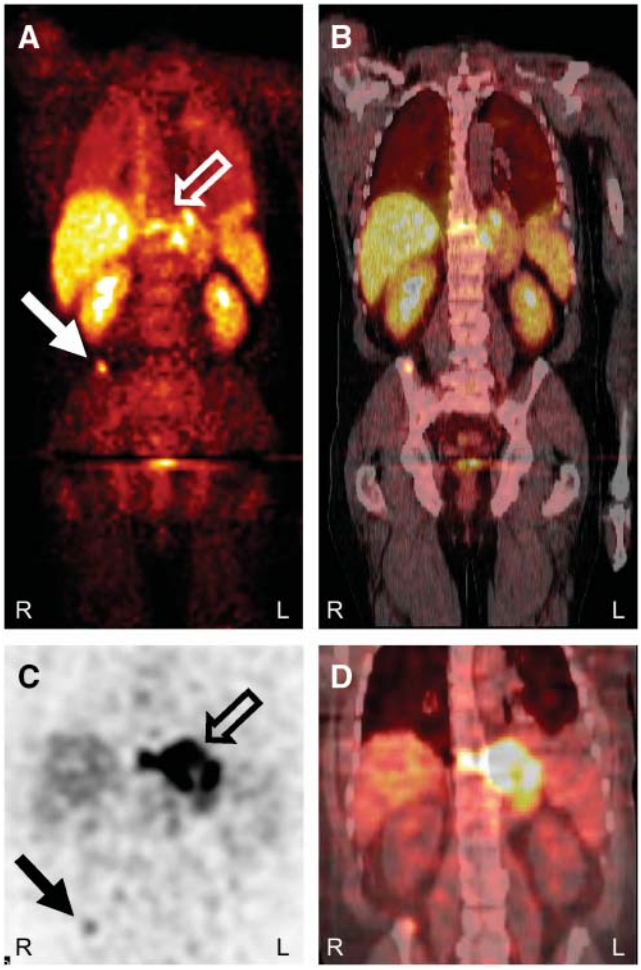

FIGURE 3. A 57-y-old man (patient GP) with metastatic paraganglioma. Primary tumor (open arrows) in left paravertebral region with involvement of 10th thoracic vertebral body and osseous metastasis in right iliac bone (solid arrows) demonstrate moderately increased ^{11}C-HED uptake in PET/CT: (A) PET, coronal slice; (B) PET/CT fusion image, coronal slice. ^{123}I-MIBG SPECT/CT: (C) SPECT, coronal slice; (D) SPECT/CT fusion image, coronal slice. Very high tracer uptake is evident in primary tumor and only faintly increased tracer uptake is seen in osseous metastasis.

comes with some disadvantages, such as limited spatial resolution; limited sensitivity in small lesions; the need for 2 or—in the case of SPECT—even more acquisition sessions with the consequent delay between the start of the examination and result; and the relatively high radiation exposure.

Feasibility of Whole-Body ^{11}C-HED PET/CT

In this study, ^{11}C-HED PET/CT using the whole-body technique was introduced as an imaging tool for tumors of the sympathetic nervous system. The study data show that whole-body ^{11}C-HED PET/CT is feasible in a clinical setting in all age group, including very young children. Similar to ^{18}F-FDG PET/CT, in toddlers sedation as well as—in rare cases—general anesthesia has to be performed for scanning (*12*). Using a state-of-the-art PET/CT scanner excellent quality attenuation-corrected images were obtained.

Comparison of ^{11}C-HED and ^{123}I-MIBG

^{11}C-HED PET/CT depicted more true-positive lesions compared with ^{123}I-MIBG SPECT/CT and clearly more compared with planar ^{123}I-MIBG scintigraphy. This led to a

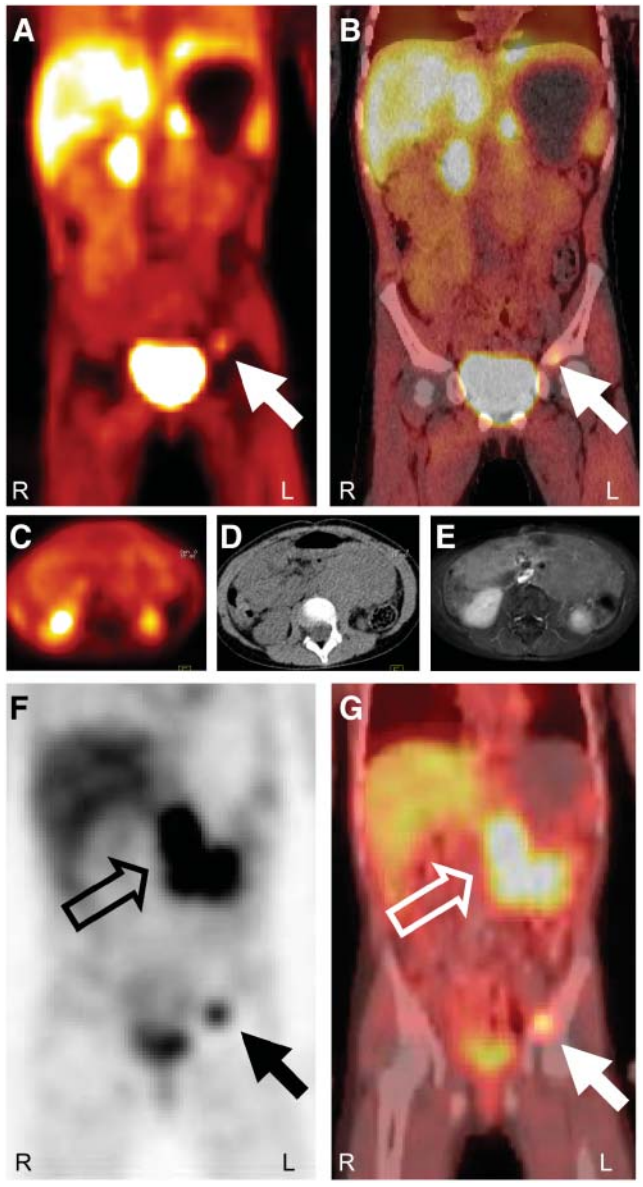

FIGURE 4. A 5-y-old girl (patient EN) who had neuroblastoma stage IV 3 y ago. Large local relapse in left upper abdomen does not demonstrate increased ^{11}C-HED uptake above surrounding tissue in PET/CT: (A) PET, coronal slice; (B) PET/CT fusion, coronal slice; (C) PET, transversal slice; (D) CT, transversal slice; (E) gadolinium-enhanced T1-weighted MRI with fat saturation, transversal slice. Osseous metastasis (solid arrows in A and B) in left hemipelvis is visible with faintly increased tracer uptake. ^{123}I-MIBG SPECT/CT: (F) SPECT, coronal slice; (G) SPECT/CT fusion, coronal slice. Local relapse (open arrows) and osseous metastasis (solid arrows) show highly increased ^{123}I-MIBG accumulation. Neuroblastoma was confirmed histologically at first diagnosis 3 y ago. In relapse situation, osseous involvement was confirmed by bone marrow puncture. Additionally, patient showed increased urinary catecholamines at first diagnosis and in relapse situation.

TABLE 5
Comparison of ^{11}C-HED Uptake and ^{123}I-MIBG Uptake: Lesion-Based Analysis

Tumor	Localization	HED > MIBG	MIBG > HED	HED = MIBG	Total
Neuroblastoma	Osseous	2	2	8	12
	Soft tissue	2	10	2	14
Pheochromocytoma	Osseous	0	0	0	0
	Soft tissue	9	2	10	21
Paraganglioma	Osseous	6	0	1	7
	Soft tissue	2	2	16	20
Ganglioneuroblastoma	Osseous	0	0	0	0
	Soft tissue	5	0	2	7
Total	Osseous	8	2	9	19
	Soft tissue	18	14	30	62
	Total	26	16	39	81

change in the therapeutic management (surgery and external radiotherapy) in 5 of 6 additional lesions in 3 of 4 examinations. Because of the limited number of patients there is a large overlap of the 95% CI of the calculated sensitivities of both tomographic methods. Therefore, ^{11}C-HED PET has at least the same high sensitivity as ^{123}I-MIBG SPECT. However, a large neuroblastoma relapse with high ^{123}I-MIBG uptake did not accumulate more ^{11}C-HED than the surrounding tissue, whereas osseous metastases in the same patient were positive in both imaging modalities. Furthermore, in 23% of soft-tissue lesions visually assessed ^{123}I-MIBG uptake was more intensive than ^{11}C-HED accumulation, whereas in 29% of soft-tissue lesions the uptake intensities were the other way round. Because the uptake mechanisms of both radiotracers are similar, an explanation could be distinct transport kinetics of both tracers in various tumors and in different tumor sites in the same patient depending on the host organ. This aspect is well known from the comparison of ^{123}I-MIBG scintigraphy with image acquisition after 4 and 24 h following injection and ^{131}I-MIBG scintigraphy with image acquisition several days after injection. Another explanation especially in small lesions may be the partial-volume effect that is more pronounced in SPECT than in PET. Further studies are necessary to elucidate this aspect. In accordance with the literature, specificity is very high, both using ^{11}C-HED PET/CT and ^{123}I-MIBG SPECT/CT, because of the specific uptake mechanism of both radiotracers (*7,13*).

Advantages of ^{11}C-HED PET/CT

Compared with ^{123}I-MIBG scintigraphy including SPECT/CT, ^{11}C-HED PET/CT has several advantages: Because of the favorable physical conditions of positron emitters, PET enables higher spatial resolution than conventional radionuclide imaging methods. This higher spatial resolution in combination with the observed selective and distinct tracer accumulation in tumors of the sympathetic nervous system enables the acquisition of excellent-quality images of these tumor entities. The value of whole-body tomography obtained by PET in comparison with the limited field of view obtained by SPECT is obvious in patients with multiple metastases. The high image quality results in the detection of more and smaller lesions. Whereas ^{123}I-MIBG scintigraphy and SPECT/CT require at least 18–24 h to achieve tumor-to-background ratios adequate for imaging, whole-body ^{11}C-HED PET/CT is completed in 1 examination within 30 min after injection. ^{123}I-MIBG scintigraphy requires at least 2 and in the case of SPECT up to 4 acquisition sessions are required. This advantage of ^{11}C-HED PET/CT is especially beneficial for children where the shorter scanning time improves comfort as well as compliance and reduces sedation (or anesthesia) time. Whole-body and especially thyroid radiation exposure are considerably lower using ^{11}C-HED PET (effective dose equivalent in adults, 1.2 mSv) compared with ^{123}I-MIBG scintigraphy (effective dose equivalent in adults, 6.0 mSv) (*5,14*).

Disadvantages and Limitations of ^{11}C-HED-PET/CT

However, ^{11}C-HED PET/CT has also some disadvantages and limitations compared with ^{123}I-MIBG scintigraphy. Because of the short half-life of ^{11}C, an on-site cyclotron is necessary. Therefore, the availability is limited. Furthermore, the on-site production for every patient is time consuming and cost intensive. Although the present study has proven that ^{11}C-HED PET/CT can be implemented in the clinical routine, the short half-life requires a rigid time schedule, which may be difficult in children or in patients who are in a poor clinical condition. Because of renal excretion during imaging, tumor manifestations next to the kidney or ureter may be missed using ^{11}C-HED PET. In this study, this potential disadvantage was obviated by ^{11}C-HED PET/CT fusion images. Furthermore, the relatively high physiologic liver uptake of ^{11}C-HED may impede the detection of small liver metastases. Some of these shortcomings may be avoided by using PET/CT with ^{18}F-labeled tracers (half-life, 110 min), such as 6-^{18}F-fluoro-3,4-dihydroxy-2-phenylalanine (^{18}F-DOPA), which has been used for imaging of a variety of neuroendocrine tumors (*15–17*). To our knowledge, there has been no study relating to ^{18}F-DOPA PET in

neuroblastoma and there are no comparison studies between ^{11}C-HED PET and ^{18}F-DOPA PET.

CONCLUSION

In summary, this study demonstrates that whole-body ^{11}C-HED PET/CT is an imaging technique, with functional images of excellent quality, that provides high sensitivity and very high specificity in the detection of tumors deriving from the sympathetic nervous system. Whole-body scanning can be performed in a clinical setting in all age groups. ^{11}C-HED PET/CT might be considered as the radionuclide imaging technique of choice if a cyclotron facility is available.

ACKNOWLEDGMENTS

The authors gratefully acknowledge the assistance of Anika Brunegraf and all other technologists of the Department of Nuclear Medicine and the Department of Clinical Radiology in performing the scans as well as Monica Trub for preparing the ^{123}I-MIBG. The authors also thank all radiologists of the Department of Clinical Radiology who have been involved in the interpretation of the low-dose CT scans and the additional morphologic imaging.

REFERENCES

1. Kushner BH. Neuroblastoma: a disease requiring a multitude of imaging studies. *J Nucl Med.* 2004;45:1172–1188.
2. Pfluger T, Schmied C, Porn U, et al. Integrated imaging using MRI and I-123-metaiodobenzylguanidine scintigraphy to improve sensitivity and specificity in the diagnosis of pediatric neuroblastoma. *AJR.* 2003;181:1115–1124.
3. Langer O, Halldin C. PET and SPET tracers for mapping the cardiac nervous system. *Eur J Nucl Med Mol Imaging.* 2002;29:416–434.
4. Rosenspire KC, Haka MS, Van Dort ME, et al. Synthesis and preliminary evaluation of C-11 metahydroxyephedrine: a false neurotransmitter agent for heart neurological imaging. *J Nucl Med.* 1990;31:1328–1334.
5. Shulkin BL, Wieland DM, Schwaiger M, et al. PET scanning with hydroxyephedrine: an approach to the localization of pheochromocytoma. *J Nucl Med.* 1992;33:1125–1131.
6. Shulkin BL, Wieland DM, Baro ME, et al. PET hydroxyephedrine imaging of neuroblastoma. *J Nucl Med.* 1996;37:16–21.
7. Trampal C, Engler H, Juhlin C, Bergström M, Langström B. Pheochromocytomas: detection with C-11 hydroxyephedrine PET. *Radiology.* 2004;230:423–428.
8. Mann GN, Link JM, Pham P, et al. [C-11]Metahydroxyephedrine and [F-18] fluorodeoxyglucose positron emission tomography improve clinical decision making in suspected pheochromocytoma. *Ann Surg Oncol.* 2006;13:187–197.
9. Franzius C, Riemann B, Vormoor J, et al. Metastatic neuroblastoma demonstrated by whole-body PET-CT using C-11-HED. *Nuklearmedizin.* 2005;44: N4–N5.
10. Pfannenberg AC, Eschmann SM, Hoger M, et al. Benefit of anatomical-functional image fusion in the diagnostic work-up of neuroendocrine neoplasms. *Eur J Nucl Med Mol Imaging.* 2003;30:835–843.
11. Moreira SGJ, Pow-Sang JM. Evaluation and management of adrenal masses. *Cancer Control.* 2002;9:326–334.
12. Franzius C, Lang K, Wormanns D, Vormoor J, Schober O. PET/CT and PET: application in pediatric oncology [in German]. *Der Nuklearmediziner.* 2004;27: 315–323.
13. Hoefnagel CA. Metaiodobenzylguanidine and somatostatin in oncology: role in the management of neural crest tumors. *Eur J Nucl Med.* 1994;21:561–581.
14. Hahn K, Fischer S. Radiation dose and radiation protection from paediatric nuclear medicine procedures [in German]. *Der Nuklearmediziner.* 2002;25: 90–100.
15. Mamede M, Carrasquillo JA, Chen CC, et al. Discordant localization of 2-[F-18]-fluoro-2-deoxy-D-glucose in 6-[F-18]-fluorodopamine- and [I-123]-metaiodobenzylguanidine-negative metastatic pheochromocytoma. *Nucl Med Commun.* 2006;27:31–36.
16. Hoegerle S, Nitzsche E, Altehoefer C, et al. Pheochromocytomas: detection with F18-DOPA whole-body PET—initial results. *Radiology.* 2002;222:507–512.
17. Becherer A, Szabó M, Karanikas G, et al. Imaging of advanced neuroendocrine tumors with F-18-FDOPA PET. *J Nucl Med.* 2004;45:1161–1167.